Anthropogenic Forcings on the Surficial Osmium Cycle

SEBASTIEN RAUCH,*,† BERNHARD PEUCKER-EHRENBRINK,‡ MALIN E. KYLANDER,§ DOMINIK J. WEISS,||,⊥ ANTONIO MARTINEZ-CORTIZAS,# DAVID HESLOP,▽ CAROLINA OLID,○ TIM M. MIGHALL,◆ AND HAROLD F. HEMOND¶

Water Environment Technology, Department of Civil and Environmental Engineering, Chalmers University of Technology, 41296 Göteborg, Sweden, Department of Marine Chemistry and Geochemistry, Woods Hole Oceanographic Institution, Woods Hole, Massachusetts 02543, Department of Geology and Geochemistry, Stockholm University, 10691 Stockholm, Sweden, Earth Science and Engineering, Imperial College London, SW72AZ London, U.K., Mineralogy, The Natural History Museum, London, SW7 5PD, London U.K., Edafologia y Quimica Agricola, Facultad de Biologia, Universidad de Santiago de Compostela-Campus Sur, 15782 Santiago, Spain, Department of Geosciences, University of Bremen, 28359 Bremen, Germany, Departament de Física Universitat Autònoma de Barcelona, E-08193 Bellaterra, Spain, School of Geosciences, University of Aberdeen, Aberdeen, AB243UF, Scotland, U.K., and Department of Civil and Environmental Engineering, Massachusetts Institute of Technology, Cambridge, Massachusetts 02139

Received June 29, 2009. Revised manuscript received October 30, 2009. Accepted November 4, 2009.

Osmium is among the least abundant elements in the Earth's continental crust. Recent anthropogenic Os contamination of the environment from mining and smelting activities, automotive catalytic converter use, and hospital discharges has been documented. Here we present evidence for anthropogenic overprinting of the natural Os cycle using a ca. 7000-year record of atmospheric Os deposition and isotopic composition from an ombrotrophic peat bog in NW Spain. Preanthropogenic Os accumulation in this area is 0.10 ± 0.04 ng m^{-2} y^{-1}. The oldest strata showing human influence correspond to early metal mining and processing on the Iberian Peninsula (ca. 4700−2500 cal. BP). Elevated Os accumulation rates are found thereafter with a local maximum of 1.1 ng m^{-2} y^{-1} during the Roman occupation of the Iberian Peninsula (ca. 1930 cal. BP) and a further increase starting in 1750 AD with Os accumulation reaching 30 ng m^{-2} y^{-1} in the most recent samples. Osmium isotopic composition ($^{187}Os/^{188}Os$) indicates that recent elevated Os accumulation results from increased input of unradiogenic Os from industrial and automotive sources as well as from enhanced deposition of radiogenic Os through increased fossil fuel combustion and soil erosion. We posit that the rapid increase in catalyst-equipped vehicles, increased fossil fuel combustion, and changes in land-use make the changes observed in NW Spain globally relevant.

Introduction

Osmium is a widely used ultratrace element in geochemical studies owing to its depletion in the Earth's crust relative to the bulk Earth and its chondritic starting material (*1, 2*), and to variations in its isotopic composition caused by the decay of ^{187}Re and ^{190}Os to ^{187}Os and ^{186}Os, respectively (*3, 4*). Applications of Os as a geochemical tracer include the quantification of global weathering processes (*5*) and the study of major geochemical reservoirs on Earth (*6*−*8*). Due to its low concentration in most environments and its limited industrial usage, few studies have focused on the environmental relevance of Os, and the biogeochemical cycling of Os in surface environments remains poorly understood. Osmium is present at concentrations <1 pg m^{-3} in the troposphere (*9*−*11*), and regional variations in $^{187}Os/^{188}Os$ in airborne particles (0.35−1.05 in New Haven, CT (*9*); 0.30−2.83 in Boston, MA (*10*); and 0.40−0.77 in Mexico City, Mexico (*11*)) and precipitation (from 0.16 in Mangalore, India to 0.44 in Montana (*12*)) indicate that multiple sources contribute to the atmospheric Os budget. High (radiogenic) $^{187}Os/^{188}Os$ values of ∼1 are characteristic of the eroding continental crust (*1*), whereas low (unradiogenic) $^{187}Os/^{188}Os$ values of 0.1−0.2 are characteristic of mantle-derived rocks and ore deposits (*13, 14*), volcanic material (*15, 16*), and undifferentiated meteorites (*17*). Anthropogenic sources are expected to have an unradiogenic isotope signature because Os is in general mined from mantle-derived ore deposits (*13, 18, 19*). Unradiogenic anthropogenic Os sources that contribute to the atmospheric Os budget include medical facilities (OsO_4 fixative for electron microscopy, emitted from hospital incinerators) (*9, 13*), automobile exhaust catalysts (Os impurities in platinum-, palladium-, and rhodium-based catalysts) (*20, 21*) and industrial metal production (smelting of Os-containing sulfide minerals) (*12, 14*).

Long-term records of atmospheric deposition such as those obtained from ombrotrophic peat bogs (*22*−*25*) enable the study of anthropogenic disturbances of the natural cycles of trace elements. Elevated Os accumulation rates over the past two decades have been determined in peat cores from Thoreau's Bog near Boston (*19*). The research presented here provides a ca. 7000 year long record of Os accumulation from an ombrotrophic peat bog in NW Spain.

Experimental Section

Peat Cores. The Os record was obtained from three cores collected at the Penido de Vello (PVO) peat bog (*23, 24, 26*), a remote site in the Xistral Mountains in NW Spain with no known anthropogenic sources in its immediate vicinity (43°32′N, 7°35′W; 780 m a.s.l., Supporting Information (SI) Figure A1). The bog is ombrotrophic, i.e., it receives minerals only through atmospheric deposition (*24*). Samples older than 1850 AD were obtained from a 292 cm core (PVO1) composed of two subcores (PVO-A: 0−245 cm, collected in 1996; PVO-B: 245−292 cm collected in 2000 approximately 25 cm apart from PVO-A). PVO1 was characterized in detail by Kylander et al. (*24*). Samples corresponding to 1850−2001 AD were obtained from a 100 cm core (PVO2) collected in

* Corresponding author phone: +46 31 772 2123; fax: +46 31 772 2128; e-mail: sebastien.rauch@chalmers.se.
† Chalmers University of Technology.
‡ Woods Hole Oceanographic Institution.
§ Stockholm University.
|| Imperial College London.
⊥ The Natural History Museum, London.
Universidad de Santiago de Compostela.
▽ University of Bremen.
○ Universitat Autònoma de Barcelona.
◆ University of Aberdeen.
¶ Massachusetts Institute of Technology.

10.1021/es901887f
Published on Web 12/09/2009

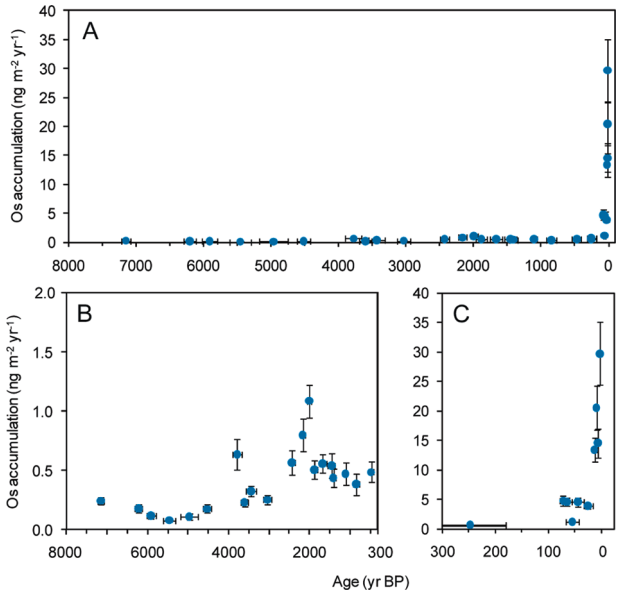

FIGURE 1. Evolution of Os accumulation at PVO (Panel A). Details of Os accumulation are provided in Panels B (age: 300−8000 year BP; accumulation rate: 0−2 ng m^{-2} y^{-1}) and C (age: 0−300 year BP; accumulation rate: 0−40 ng m^{-2} y^{-1}). Age is presented in year before present (BP) with 2001 AD as present. Error bars represent 2 standard deviations. Error bars represent 2 standard deviations for ages (inferred from the age model) and 5% analytical error (inferred from the analysis of homogeneous geological reference materials) including uncertainty resulting from dating error (inferred from the age model) for Os accumulation.

2001. Details of the dating methods used to establish the chronologies of PVO cores are provided in the SI. A coal sample from a power plant in Northern Spain was also analyzed for Os concentration and $^{187}Os/^{188}Os$.

Osmium Analysis. Osmium was isolated from a few grams of peat by NiS fire assay (*27*) after the addition of a tracer solution enriched in ^{190}Os. Pooling of multiple samples was necessary for some depth intervals to obtain enough material for Os determination. The method preconcentrates Os into a NiS bead, which is subsequently dissolved in HCl. Residual HCl-insoluble particles were collected on filters that were dissolved in hot concentrated HNO_3. Volatile OsO_4 formed during the dissolution was sparged (*28*) into the torch of a multicollector inductively coupled plasma-mass spectrometer (MC ICP-MS, NEPTUNE, ThermoElectron). A multidynamic data acquisition routine involving three continuous dynode electron multipliers allowed for correction of variable multiplier efficiencies and instrumental mass fractionation. Osmium concentrations were calculated using the $^{187}Os/^{188}Os$, $^{190}Os/^{188}Os$ and $^{192}Os/^{188}Os$ ratios. The relative internal standard deviation of $^{187}Os/^{188}Os$, including blank correction, was always smaller than 2.6%. The precision, accuracy and procedural blanks of the analytical method are documented in the SI, as well as by Peucker-Ehrenbrink et al. (*29*) and Rauch et al. (*10*). Osmium accumulation rates are calculated from Os concentrations and peat accumulation rates inferred from peat chronology. Results are presented as average values ±2 standard deviations when a period is described that is represented by several data points. Error bars in the figures are described in respective captions. The uncertainty resulting from uneven Os distribution in peat could not be rigorously calculated, but the analysis of replicate samples ($n = 2$) at 14 cm depth indicates that Os is relatively homogeneously distributed in peat, yielding Os concentrations of 8.4 and 10.6 pg g^{-1} and $^{187}Os/^{188}Os$ of 0.91 and 0.86, respectively. Osmium concentrations and $^{187}Os/^{188}Os$ of potential natural and anthropogenic Os sources are summarized in Table 2.

Complementary Data. Lead isotopic composition (*24*), ash content (determined by ashing at 450 °C and presented as % of dry weight), and rare earth element (REE) concentrations (determined by quadrupole ICP-MS after acid digestion with HNO_3, HF, and $HClO_4$) at PVO as well as tree pollen at the nearby Peña da Cadela peat bog (*30*) complement the Os record. REE are presented as La/Lu, with La representing light REE (LREE) and Lu representing heavy REE (HREE). Chondrite-normalized REE concentrations can be used to differentiate between crustal and mantle-derived rocks, as upper crustal rocks typically are enriched in LREE vs HREE, whereas mantle-derived rocks often show complementary depletion (*31*). Enrichment of LREE vs HREE has also been reported in top-soil (*32*). Temporal changes in La/Lu in the peat records therefore likely provide insights into potential sources of mineral dust, with increasing ratios corresponding to an increase in the relative contribution of upper crustal dust or soil.

Results and Discussion

Evolution of the Os Record at PVO. Osmium concentrations, accumulation rates and $^{187}Os/^{188}Os$ vary from 4.1 to 35 pg Os g^{-1}, 0.14−30 ng Os m^{-2} y^{-1}, and 0.31 to 0.91, respectively (Figures 1−3, Table 1). Sharp gradients in Os concentrations and accumulation rates correspond to historic trends suggesting that Os is immobile at the studied scale. Based on variations of Os accumulation rates (Figure 1) and inverse Os concentration against $^{187}Os/^{188}Os$ (Figure 3B) the peat record can be divided into three phases.

Phase I, Preanthropogenic Os sources (ca. 4700−6000 cal. BP). Preanthropogenic Os deposition (taken to be ca. 4700−6000 cal. BP based on Os accumulation rates, isotopic composition and ash content) is characterized by low accumulation rates (0.10 ± 0.04 ng m^{-2} y^{-1}) and relatively constant isotopic composition. The average $^{187}Os/^{188}Os$ of 0.70 ± 0.16 and the mixing trend observed in Figure 3B are indicative of contributions from both radiogenic and unradiogenic sources. Potential radiogenic contributors include input from local erosion (the local geology is dominated by radiogenic Variscan mica-granites and underlying sediments with a depositional age of ca. 7100 ± 80 cal. BP have an $^{187}Os/^{188}Os$ of 0.84) and Saharan dust (supported by Pb isotope

TABLE 1. Osmium Accumulation Rates and Isotopic Composition at PVO during phases I−III[a]

phase	age/date	accumulation rates (ng Os m^{-2} y^{-1})	$^{187}Os/^{188}Os$
phase I, preanthropogenic sources	4700−6000 cal. BP	0.10 ± 0.04	0.70 ± 0.16
phase II, early anthropogenic sources	4700−200 cal. BP	0.5 ± 0.5	0.54 ± 0.25
phase IIa, copper and bronze ages	4700−2500 cal. BP	0.3 ± 0.2	0.53 ± 0.28
phase IIb, iron age and Roman occupation	1900−2500 cal. BP	0.8 ± 0.3	0.41 ± 0.21
phase IIc, intermediate	1900−200 cal. BP	0.5 ± 0.1	0.54 ± 0.15
phase III, industrial and recent sources	1750 AD to 2001 AD	9 (19)	0.73 ± 0.34
phase IIIa, industrial period	1750 AD to 1989 AD	2.9 (3.9)	0.70 ± 0.38
phase IIIb, recent period	1989 AD to 2001 AD	20 ± 15	0.78 ± 0.28

[a] Results are presented as average values ±2 standard deviations (error in brackets when it exceeds average value).

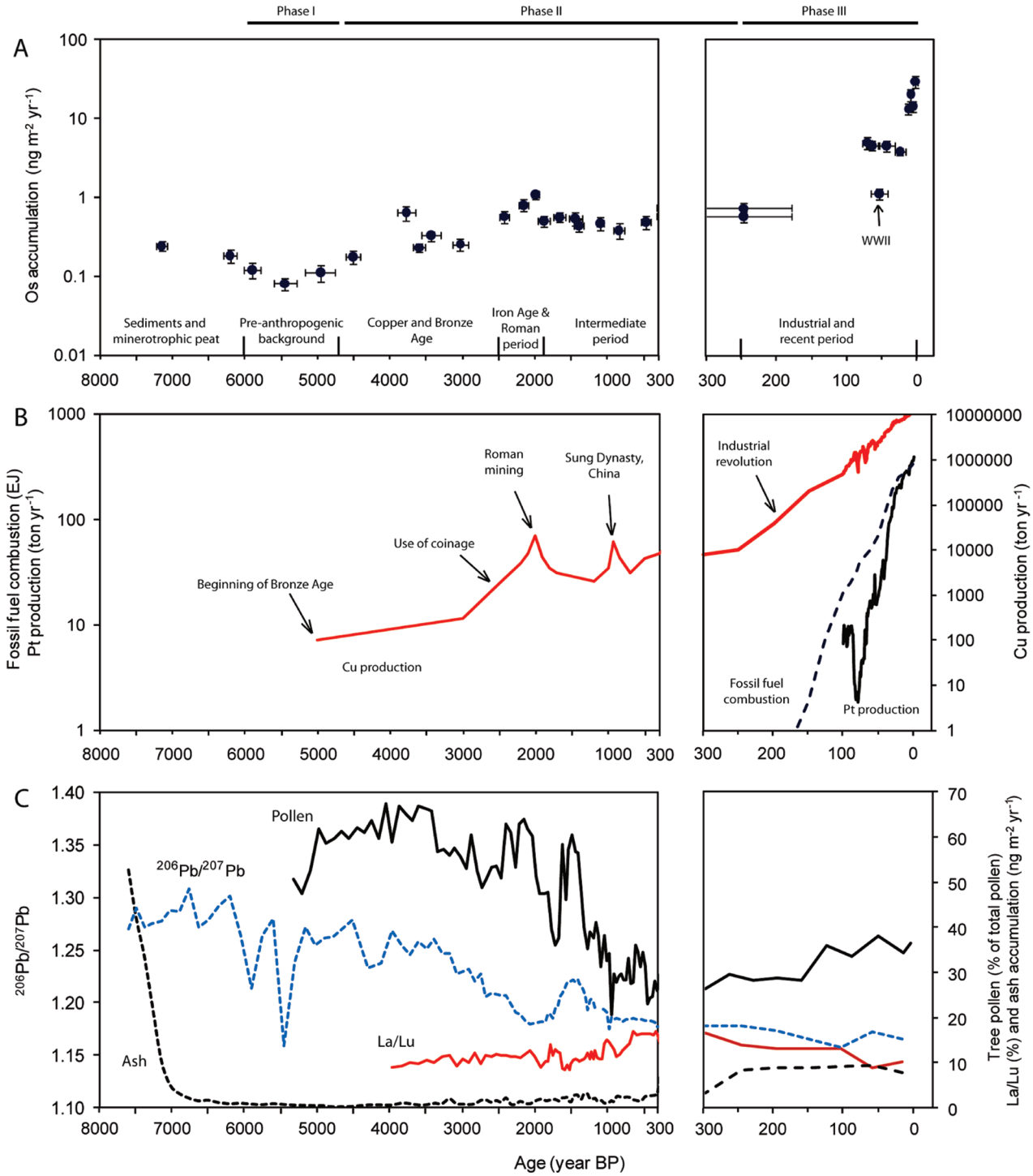

FIGURE 2. Comparison of Os accumulation with global Cu production (*37, 41*), global platinum group element (PGE) production (*41*), fossil fuel combustion (*42*), tree pollen at a nearby peat bog (*30*), Pb isotopes (*24*), ash accumulation, and rare earth elements (La/Lu). The *x*-axis is a continuum but with a different scaling for the last 300 years.

data (*24*); Saharan dust has an $^{187}Os/^{188}Os$ of 1.2 (*33*)), whereas less radiogenic sources may include aeolian dust from the ultramafic Cabo Ortegal platiniferous deposit ca. 35 km west of PVO (*34*) or volcanic emissions with $^{187}Os/^{188}Os$ of <0.4 (*15, 16*).

Phase II, Early Anthropogenic Os Sources (ca. 4700−200 cal. BP). This phase is defined by increasing Os accumulation rates and a well-defined linear mixing array (Figure 3B) between Os-poor radiogenic and Os-rich unradiogenic sources. Osmium accumulation rates first increased during the Copper and Bronze Ages with the onset of metal mining activities in Europe, including mining on the Iberian Peninsula (phase IIa, ca. 4700−2500 cal. BP) (*35*). The expansion of mining activities during the Iron Age and Roman occupation of the Iberian Peninsula (phase IIb, ca. 1900−2500 cal. BP) coincides with a further increase in Os accumulation rates to a maximum of 1.1 ng m^{-2} y^{-1} around ca. 1930 ± 60 cal. BP. As neither the pre-Roman inhabitants of the Iberian Peninsula nor its Roman occupants are known to have explicitly mined or used Os, we hypothesize that Os was emitted as a byproduct of Cu production from sulfide deposits, including the Rio Tinto deposit 600 km south of PVO, where Cu has been mined since 5000 cal. BP (*35*). This hypothesis is consistent with the chalcophile behavior of Os

TABLE 2. Osmium Concentrations and $^{187}Os/^{188}Os$ of Potential Os Sources

material	Os concentrations(ng/g)	$^{187}Os/^{188}Os$	references
continental crust	0.03	1.4	*1*
Saharan dust		1.2	*33*
volcanic emissions		0.14	*15, 16*
cosmic dust	500	0.13	*17*
sea water	0.00001	1.06	*8*
fossil fuel combustion (coal and petroleum)	0.01−285	0.6−6.0	(*14, 43, 44,* this study)
Metal Production Activities			
Metal Sulfide Ores			
PGE ores (Bushveld, South Africa)	20−50	0.14−0.20	*45*
Noril'sk ores (Russia)	0.8−600	0.1−0.3	*46*
Sudbury ores (Canada)	0.03−89	0.9−15	*47*
Iberian Pyrite Belt ores (Spain)	0.05−0.7	0.4−29	*48*
iron ores (Sweden)	0.02−0.05	1.6−7.9	*14*
chromites	0.5−68	0.13	*14*
molybdenites	10−100	up to 7000	*14*
automobile catalytic converters	0.006−3	0.1−0.4	*14, 20*
tunnel dust (representative of automobile emissions)	1.2	0.27	*49*
hospital waste		0.1−0.2	*18*

and is supported by the good temporal correlation between Os accumulation at PVO and global Cu production (*36*) (Figure 2B). This hypothesis is also consistent with the pattern of atmospheric transport of pollution from SW Spain inferred from source tracing based on Pb isotopes (Figure 2C). Lead isotope data show a decline in $^{206}Pb/^{207}Pb$ centered around 2000 cal. BP which was attributed to Roman mining in SW Spain (*24*). Mining operations in SW Spain were abandoned following the end of Roman occupation and were not resumed again until the 19th century. The decline in accumulation rates to 0.5 ± 0.2 ng m^{-2} y^{-1} in peat layers above that corresponding to Roman Os accumulation in the PVO bog reflects this decline in mining activities. The only exception to this trend is the high accumulation rate of 0.6 ng m^{-2} y^{-1} at ca. 3720 ± 120 cal. BP. This local maximum may result from volcanic emissions; a global climatic disturbance that occurred in the 17th Century BC is attributed to volcanic eruptions, possibly including the Minoan eruption of Thera, Greece, the Avellino eruption of Mount Vesuvius, Italy, and the eruption of Mount Aniakchak, AK (*37*).

Phase III, Industrial and Other Recent Anthropogenic Os Sources (ca. 1750 AD to 2001 AD). A further increase in Os accumulation rates begins in ca. 1750 ± 70 AD and corresponds to an increase in industrial activities, including mining, on the Iberian Peninsula (Figure 1). Phase III is also marked by an increase in the use of fossil fuels (Figure 2B). Accumulation rates reach values of 3.6−5.3 ng m^{-2} y^{-1} in 1920−1985 AD, except for a lower accumulation in 1947 ± 12 AD which is possibly caused by a decrease in industrial activities in Europe during World War II. Osmium accumulation rates increased more rapidly after ca. 1989 ± 5 AD, and reached a maximum of ~300 fold preanthropogenic accumulation rates (30 ng m^{-2} y^{-1}) in 2001 AD despite the fact that mining activities on the Iberian Peninsula decreased during this period and Cu mining in SW Spain ceased in 1984 AD (*38*). It is interesting to note that current Os accumulation rates at PVO are higher than those observed in Thoreau's Bog near Boston, MA (5 ng m^{-2} y^{-1} (*19*)) and in New Haven, CT (5 ng m^{-2} y^{-1} (*9*)), despite the less industrialized surroundings of the PVO site.

The release of Os from automobile exhaust catalysts may be one major cause of the recent increase in Os accumulation rates observed at PVO. Platinum-, Pd-, and Rh-based automobile exhaust catalysts were introduced in Europe in the late 1980s and were mandated on new gasoline-powered light duty vehicles in the European Union in 1993, resulting in a rapid increase in catalyst numbers. Catalysts contain significant amounts of Os, which is emitted as volatile OsO_4 (*20*) and is readily reduced and sorbed upon contact with airborne particles (*39*) and organic matter. The mining, smelting, and refining of platinum group elements (PGE) used in catalysts has been suggested as a possible source of Os (*12*). However, the correspondence between the onset of increased Os accumulation rates and the local introduction of catalysts indicates that automobile emissions are a more important Os source at PVO.

If the observed increase in Os accumulation rates was caused solely by enhanced input from unradiogenic sources, then the $^{187}Os/^{188}Os$ of the bulk peat should decline. Isotope mixing relationships for phase III samples show that this is not the case, however (Figure 3B). Phase III samples deviate from the two-component mixing line defined by phase I and II samples, and the most recent (phase IIIb) samples lie on a new two-component mixing line with a steeper slope. The isotope mixing diagram indicates that radiogenic and unradiogenic sources contributed to the most recent increase in Os accumulation rates. An increased radiogenic contribution points to fossil fuel combustion or to changes in erosion rates, the latter possibly linked to increased agricultural activity and/or desertification in Southern Europe. Fossil fuels, whose combustion soared after the industrial revolution (ca. 200 cal. BP, Figure 2B), can have relatively high $^{187}Os/^{188}Os$ values (Table 2) and may therefore contribute to the observed deviation from the original two-component mixing line. In contrast, the increase in tree pollen abundance (i.e., increased forest cover resulting in less erosion) and decrease in La/Lu (upper crustal sources are characterized by a relatively high La/Lu ratio; we note that an enrichment of LREE vs HREE observed at a Swiss peat bog since the beginning of the 19th century and attributed to industrial emissions (*40*) is not observed at PVO) during phase III suggest that fossil fuel combustion is a more important contributor to the radiogenic component than aeolian dust.

Observed variations in Os concentrations, accumulation rates and $^{187}Os/^{188}Os$ are consistent with multiple Os sources, and provide constraints on the interpretation of the peat record. Prior to ca. 200 cal. BP (phases I and II) the profile defines a 2-component mixing line between an Os-poor radiogenic component (aeolian dust from local erosion or from the Sahara) and an Os-rich unradiogenic component (aeolian dust from a less radiogenic source region, volcanic emissions or mining activities). However, data deviate from this 2-component mixing line after this date, as higher Os concentrations are found along with relatively radiogenic $^{187}Os/^{188}Os$ ratios in phase III (Figure 3B). The most recent

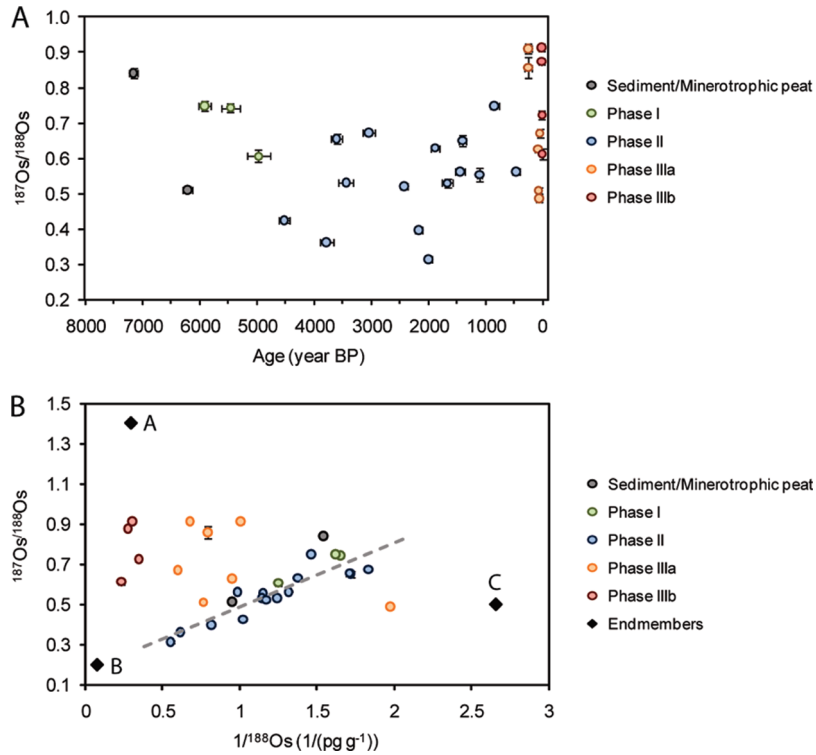

FIGURE 3. Evolution of Os isotopic composition at PVO (Panel A) and $^{187}Os/^{188}Os$ vs $1/^{188}Os$ (Panel B). A deviation from the two component mixing line in phases I and II is observed in phase III. For $^{187}Os/^{188}Os$, the uncertainty represents the analytical error (2 standard deviations, estimated during sample analysis). Endmembers used in the three-component model are presented in Panel B.

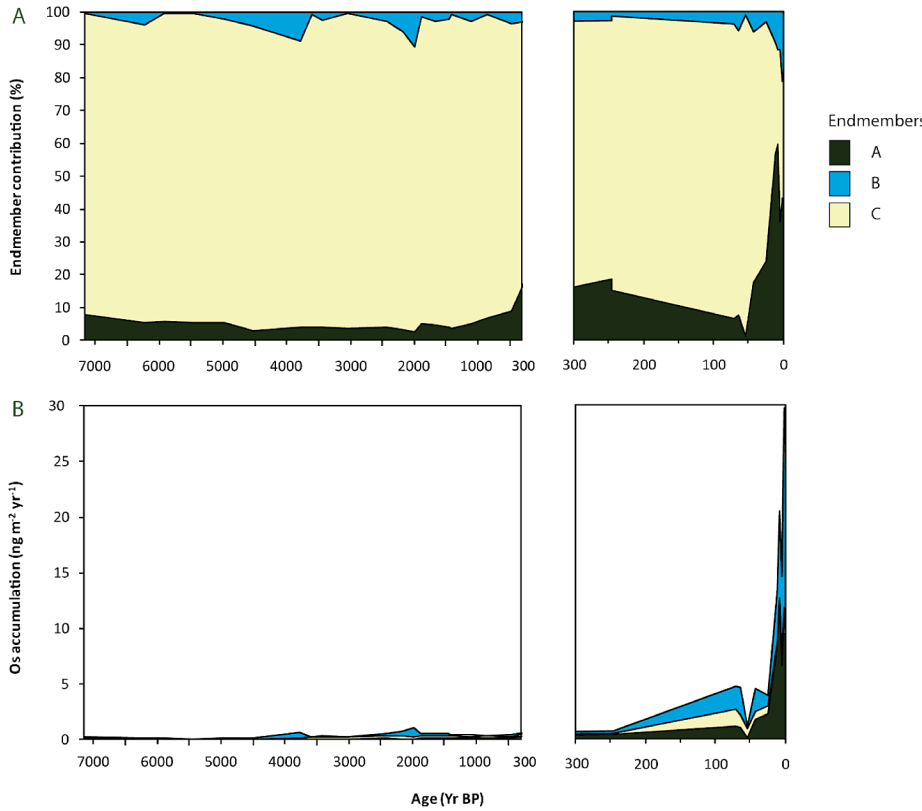

FIGURE 4. (A) Relative endmember contribution inferred from the three-component isotope mixing model. (B) Os accumulation rates of various endmembers. A: radiogenic endmember (30 pg Os/g, $^{187}Os/^{188}Os = 1.4$); B: unradiogenic endmember (100 pg Os/g, $^{187}Os/^{188}Os = 0.2$); C: intermediate endmember (3 pg Os/g, $^{187}Os/^{188}Os = 0.5$). The *x*-axis is a continuum but with a different scaling for the last 300 years.

samples define a two-component mixing line with steeper slope than the pre- and early-anthropogenic mixing line.

Three Component Isotope Mixing Model. The isotope mixing relationships can be used to model the relative contributions from various endmembers. The experimental data indicate that at least three endmembers are needed to explain the observed distribution. While it might appear attractive to define the endmembers as end-points of two 2-component mixing lines, we choose here to define the three endmembers as vertices of a triangle that encloses all data points (Figure 3B). This ensures that the three-component mixing calculation yields only positive fractional contributions. It also means that we are treating the radiogenic endmember of the correlation line with the shallow slope (phase I and II) as a mixture of an even more radiogenic endmember (A) with a less radiogenic endmember (C) at relatively constant mixing ratios. We further assume that the isotopic composition of the sources, but not their relative contributions to the PVO site, has remained constant for the past 7000 years. Two of the vertices are compositionally similar to the end-points of the steep (phase IIIb) mixing line and the intersection of the phase III and phase II mixing lines. Endmember A (30 pg Os g^{-1}, $^{187}Os/^{188}Os = 1.4$) lies close to the radiogenic end-point of the steep (phase III) two-component mixing line. Its isotope composition has been chosen to coincide with the average value of the eroding upper continental crust (*1*). As mentioned earlier, fossil fuels may have relatively high $^{187}Os/^{188}Os$ and possibly contribute to this endmember. Although emissions from molybdenite smelters release Os with very high $^{187}Os/^{188}Os$ (*14*) and constitute a potential radiogenic endmember, the dearth of such smelters in Europe makes them less likely to contribute to Os deposition at PVO. Based on the intersection of the two two-component mixing lines near the origin of the isotope mixing diagram, the $^{187}Os/^{188}Os$ of the unradiogenic, Os-rich endmember B has to be less than 0.25, and its Os concentration has to be higher than about 80 pg g^{-1}. We assign a $^{187}Os/^{188}Os$ value of 0.2 and an Os concentration of 100 pg g^{-1} to this endmember. The third endmember, C, has low Os concentrations and an intermediate $^{187}Os/^{188}Os$. We choose an Os concentration of 3 pg g^{-1} and a $^{187}Os/^{188}Os$ value of 0.5, but acknowledge that the Os concentration could be significantly lower, and that the $^{187}Os/^{188}Os$ could be slightly more or less radiogenic than 0.5. This endmember could represent an Os-poor mineral phase (aeolian quartz or carbonate) or a coal-combustion product (local coal has a $^{187}Os/^{188}Os$ of ~0.5) with low Os concentrations. In spite of significant uncertainty in the exact definition of the endmembers we emphasize that the basic conclusions are not significantly affected by the choice of endmember composition.

Figure 4A shows the relative contributions of these three endmembers to the PVO peat record. Most importantly, the model successfully reconciles the observation that Os concentrations and accumulation rates increase toward the top of the core, whereas the $^{187}Os/^{188}Os$ do not change significantly. This feature results from concomitant increases in both the Os-rich unradiogenic (catalytic converters and other industrial uses) and the moderately Os-rich radiogenic (aeolian dust, coal combustion) endmember contributions.

Osmium accumulation rates inferred from relative endmember contributions and assumed Os concentrations support the interpretation that important changes in the source of Os at PVO have occurred since ca. 4500 cal. BP (Figure 4B). Enhanced accumulation of unradiogenic Os (endmember B) occurred in ca. 3600−4500 cal. BP, ca. 1800−3000 cal. BP, and after ca. 1750 AD. In contrast, the accumulation rate of unradiogenic (endmember A) and intermediate (endmember C) Os consistently increased starting from ca. 4500 cal. BP. After ca. 1750 AD, a more rapid increase in Os accumulation is observed for all three endmembers. The accumulation of the intermediate Os endmember decreases after ca. 1950 AD, and Os accumulation is dominated by both radiogenic and unradiogenic endmembers after ca. 1977 AD. These observations are consistent with Os emissions from early metal mining and smelting on the Iberian Peninsula, from metal production industries in ca. 1750−1980 AD, from fossil fuel combustion after 1750 AD and from automobile catalyst emissions starting in the 1980s AD, as well as increasing erosion resulting from land use changes and desertification starting from ca. 1500 cal. BP (concomitant increase in the radiogenic Os component, decrease in tree pollen and increase in La/Lu support an erosion source from ca. 1500 cal. BP to ca. 200 cal. BP; as fossil fuel combustion increase after ca. 200 cal. BP, the contribution from erosion becomes less significant).

Implications of Observed Changes. The PVO record provides evidence for the anthropogenic overprinting of the natural cycle of Os. However, because human use of Os is limited to a few specific applications, little of the anthropogenic Os input to the atmosphere results from deliberate use of Os. The largest anthropogenic effects appear to be those that release Os as a byproduct or impurity (metal production activities, automobile exhaust catalysts, fossil fuel combustion), or result in increased Os input from natural sources, such as soil erosion. Due to the rapidly increasing number of catalyst-equipped vehicles, the combustion of fossil fuels and changes in land use, as well as the atmospheric dispersion of emitted Os, the changes observed at PVO are of global relevance. Although current atmospheric Os concentrations (*9*−*11*) are not thought to be a risk factor for human health, they may affect the use of Os in geochemical studies in surface environments with low intrinsic Os concentrations. Chen et al. (*12*) provide one possible example for such anthropogenic contamination finding that the $^{187}Os/^{188}Os$ of water in the mixed layer of the Atlantic Ocean is less radiogenic than that of deep waters. We hypothesize that anthropogenic Os emissions are larger than previously estimated based on Os isotopic composition or emission inventories (*12*) because only unradiogenic Os sources are considered. Further studies of unradiogenic and radiogenic anthropogenic emissions and anthropogenically enhanced natural processes are needed to determine their impact on the surficial Os cycle.

Acknowledgments

We are thankful to Tracy Atwood, Lary Ball, and David Schneider of the Woods Hole Oceanographic Institution for their assistance with Os analyses in the NSF-supported WHOI ICPMS Facility (grants EAR-03181137 and EAR-0651366). We acknowledge funding from the Spanish Ministerio de Educacion y Ciencia (REN200-09228-C02-01) and Conselleria de Innovacion, Industria e Comercio, Xunta de Galicia (PGIDT-03PXIB20002PR) for geochemical studies at PVO, and from the Knut and Alice Wallenberg Foundation and the Alliance for Global Sustainability for research on platinum group elements.

Supporting Information Available

Map of the sampling site, the data set and descriptions of peat characterization, the age model, and analytical performance. This material is available free of charge via the Internet at http://pubs.acs.org.

Literature Cited

(1) Peucker-Ehrenbrink, B.; Jahn, B. M., Rhenium-osmium isotope systematics and platinum group element concentrations: Loess and the upper continental crust. *Geochem., Geophys., Geosyst.* **2001**, *2*, DOI: 10.1029/2001GC000172.

(2) Peucker-Ehrenbrink, B.; Ravizza, G. The effects of sampling artifacts on cosmic dust flux estimates: A reevaluation of nonvolatile tracers (Os, Ir). *Geochim. Cosmochim. Acta* **2000**, *64*, 1965–1970.

(3) Allègre, C. J.; Luck, J. M. Osmium isotopes as petrogenetic and geological tracers. *Earth Planet. Sci. Lett.* **1980**, *48*, 148–154.
(4) Shirey, S. B.; Walker, R. J. The Re-Os isotope system in cosmochemistry and high-temperature geochemistry. *Annu. Rev. Earth Planet. Sci.* **1998**, *26*, 423–500.
(5) Ravizza, G.; Norris, R. N.; Blusztajn, J. An osmium isotope excursion associated with the late Paleocene thermal maximum: Evidence of intensified chemical weathering. *Paleoceanography* **2001**, *16*, 155–163.
(6) Saal, A. E.; Rudnick, R. L.; Ravizza, G. E.; Hart, S. R. Re-Os isotope evidence for the composition, formation and age of the lower continental crust. *Nature* **1998**, *393*, 58–61.
(7) Meisel, T.; Walker, R. J.; Morgan, J. W. The osmium isotopic composition of the Earth's primitive upper mantle. *Nature* **1996**, *383*, 517–520.
(8) Peucker-Ehrenbrink, B.; Ravizza, G. The marine osmium isotope record. *Terra Nova* **2000**, *12*, 205–219.
(9) Williams, G. A.; Turekian, K. K. Atmospheric supply of osmium to the oceans. *Geochim. Cosmochim. Acta* **2002**, *66*, 3789–3791.
(10) Rauch, S.; Hemond, H. F.; Peucker-Ehrenbrink, B.; Ek, K. H.; Morrison, G. M. Platinum group element concentrations and osmium isotopic composition in urban airborne particles from Boston, Massachusetts. *Environ. Sci. Technol.* **2005**, *39*, 9464–9470.
(11) Rauch, S.; Peucker-Ehrenbrink, B.; Molina, L. T.; Molina, M. J.; Ramos, R.; Hemond, H. F. Platinum group elements in airborne particles in Mexico City. *Environ. Sci. Technol.* **2006**, *40*, 7554–7560.
(12) Chen, C.; Sedwick, P. N.; Sharma, M. Anthropogenic osmium in rain and snow reveals global-scale atmospheric contamination. *Proc. Natl. Acad. Sci. U. S. A.* **2009**, *106*, 7724–7728.
(13) Esser, B. K.; Turekian, K. K. Anthropogenic osmium in coastal deposits. *Environ. Sci. Technol.* **1993**, *27*, 2719–2724.
(14) Rodushkin, I.; Engstrom, E.; Sorlin, D.; Ponter, C.; Baxter, D. C. Osmium in environmental samples from Northeast Sweden Part II.Identification of anthropogenic sources. *Sci. Total Environ.* **2007**, *386*, 159–168.
(15) Krähenbühl, U.; Geissbühler, M.; Bühler, F.; Eberhardt, P.; Finnegan, D. L. Osmium isotopes in the aerosols of the mantle volcano Mauna-Loa. *Earth Planet. Sci. Lett.* **1992**, *110*, 95–98.
(16) Alves, S.; Schiano, P.; Allégre, C. J. Rhenium-osmium isotopic investigation of Java subduction zone lavas. *Earth Planet. Sci. Lett.* **1999**, *168*, 65–77.
(17) Luck, J. M.; Allegre, C. J. Re-187-Os-187 systematics in meteorites and cosmochemical consequences. *Nature* **1983**, *302*, 130–132.
(18) Ravizza, G. E.; Bothner, M. H. Osmium isotopes and silver as tracers of anthropogenic metals in sediments from Massachusetts and Cape Cod bays. *Geochim. Cosmochim. Acta* **1996**, *60*, 2753–2763.
(19) Rauch, S.; Hemond, H. F.; Peucker-Ehrenbrink, B. Source characterisation of atmospheric platinum group element deposition into an ombrotrophic peat bog. *J. Environ. Monit.* **2004**, *6*, 335–343.
(20) Poirier, A.; Gariepy, C. Isotopic signature and impact of car catalysts on the anthropogenic osmium budget. *Environ. Sci. Technol.* **2005**, *39*, 4431–4434.
(21) Fritsche, J.; Meisel, T. Determination of anthropogenic input of Ru, Rh, Pd, Re, Os, Ir, and Pt in soils along Austrian motorways by isotope dilution ICP-MS. *Sci. Total Environ.* **2004**, *325* (1−3), 145–154.
(22) Shotyk, W.; Weiss, D.; Appleby, P. G.; Cheburkin, A. K.; Frei, R.; Gloor, M.; Kramers, J. D.; Reese, S.; Van der Knaap, W. O. History of atmospheric lead deposition since 12,370 C-14 yr BP from a peat bog, Jura Mountains, Switzerland. *Science* **1998**, *281*, 1635–1640.
(23) Martinez Cortizas, A.; Pontevedra Pombal, X.; Garcia-Rodeja, E.; Novoa Munoz, J. C.; Shotyk, W. Mercury in a Spanish peat bog: Archive of climate change and atmospheric metal deposition. *Science* **1999**, *284*, 939–942.
(24) Kylander, M. E.; Weiss, D. J.; Cortizas, A. M.; Spiro, B.; Garcia-Sanchez, R.; Coles, B. J. Refining the pre-industrial atmospheric Pb isotope evolution curve in Europe using an 8000 year old peat core from NW Spain. *Earth Planet. Sci. Lett.* **2005**, *240*, 467–485.
(25) Bindler, R. Estimating the natural background atmospheric deposition rate of mercury utilizing ombrotrophic bogs in southern Sweden. *Environ. Sci. Technol.* **2003**, *37*, 40–46.
(26) Martinez Cortizas, A.; Pontevedra Pombal, X.; Movoa Munoz, J. C.; Garcia-Rodeja, E. Four thousand years of atmospheric Pb, Cd, and Zn deposition recorded by the ombrotrophic peat bog of Penido Vello (northwestern Spain). *Water, Air, Soil Pollut.* **1997**, *100* (3−4), 387–403.
(27) Ravizza, G. Pyle, PGE and Os isotopic analyses of single sample aliquots with NiS fire assay preconcentration. *Chem. Geol.* **1997**, *141*, 251–268.
(28) Hassler, D. R.; Peucker-Ehrenbrink, B.; Ravizza, G. E. Rapid determination of Os isotopic composition by sparging OsO_4 into a magnetic-sector ICP-MS. *Chem. Geol.* **2000**, *166*, 1–14.
(29) Peucker-Ehrenbrink, B.; Bach, W.; Hart, S. R.; Blusztajn, J. S.; Abbrussese, T., Rhenium-osmium isotope systematics and platinum group element concentrations in oceanic crust from DSDP/OPD Sites 504 and 417/418. *Geochem., Geophys., Geosyst.* **2003**, *4*, DOI: 10.1029/2003GC000414.
(30) Martinez Cortizas, A.; Mighall, T.; Pontevedra Pombal, X.; Novoa Munoz, J. C.; Peiteado Varela, E.; Pineiro Rebolo, R. Linking changes in atmospheric dust deposition, vegetation change and human activities in northwest Spain during the last 5300 years. *Holocene* **2005**, *15*, 698–706.
(31) Geochemistry and Mineralogy of rare earth elements. In *Reviews in Mineralogy*; Lipin, B. R.; Mckay, G. A., Eds.; Mineralogical Society of America: Chantilly, VA, 1989; Vol. 21, pp 348.
(32) Tyler, G. Rare earth elements in soil and plant systems. *Plant Soil* **2004**, *267*, 191–206.
(33) Grousset, F. E.; Biscaye, P. E. Tracing dust sources and transport patterns using Sr, Nd and Pb isotopes. *Chem. Geol.* **2005**, *222* (3−4), 149–167.
(34) Moreno, T.; Gibbons, W.; Prichard, H. M.; Lunar, R. Platiniferous chromitite and the tectonic setting of ultramafic rocks in Cabo Ortegal, NW Spain. *J. Geol. Soc.* **2001**, *158*, 601–614.
(35) Nocete, F. The first specialised copper industry in the Iberian peninsula: Cabezo Jure (2900−2200 BC). *Antiquity* **2006**, *80*, 646–657.
(36) Hong, S. M.; Candelone, J. P.; Soutif, M.; Boutron, C. F. A reconstruction of changes in copper production and copper emissions to the atmosphere during the past 7000 years. *Sci. Total Environ.* **1996**, *188*, 183–193.
(37) Vogel, J. S.; Cornell, W.; Nelson, D. E.; Southon, J. R. Vesuvius Avellino, one possible source of 17th-century-BC climatic disturbances. *Nature* **1990**, *344*, 534–537.
(38) Davis, R. A.; Welty, A. T.; Borrego, J.; Morales, J. A.; Pendon, J. G.; Ryan, J. G. Rio Tinto estuary (Spain): 5000 years of pollution. *Environ. Geol.* **2000**, *39*, 1107–1116.
(39) Smith, I. C.; Carson, B. L.; Ferguson, T. L. Osmium: an appraisal of environmental exposure. *Environ. Health Perspect.* **1974**, *8*, 201–213.
(40) Krachler, M.; Mohl, C.; Emons, H.; Shotyk, W. Two thousand years of atmospheric rare earth element (REE) deposition as revealed by an ombrotrophic peat bog profile, Jura Mountains, Switzerland. *J. Environ. Monit.* **2003**, *5*, 111–121.
(41) USGS Historical Statistics for Mineral and Material Commodities in the United States. http://minerals.usgs.gov/ds/2005/140/.
(42) Grubler, A., Energy transitions. In *Encyclopedia of Earth*, Cleveland, C. J., Ed.; Environmental Information Coalition, National Council for Science and the Environment: Washington, D.C., 2008.
(43) Selby, D.; Creaser, R. A.; Fowler, M. G. Re-Os elemental and isotopic systematics in crude oils. *Geochim. Cosmochim. Acta* **2007**, *71*, 378–386.
(44) Selby, D.; Creaser, R. A. Direct radiometric dating of hydrocarbon deposits using rhenium-osmium isotopes. *Science* **2005**, *308*, 1293–1295.
(45) McCandless, T. E.; Ruiz, J. Osmium isotopes and crustal sources for platinum-group mineralization in the Bushveld Complex, South-Africa. *Geology* **1991**, *19*, 1225–1228.
(46) Walker, R. J.; Morgan, J. W.; Hanski, E. J.; Smolkin, V. F. Re-Os systematics of Early Proterozoic ferropicrites, Pechenga Complex, northwestern Russia: Evidence for ancient Os-187-enriched plumes. *Geochim. Cosmochim. Acta* **1997**, *61*, 3145–3160.
(47) Morgan, J. W.; Walker, R. J.; Horan, M. F.; Beary, E. S.; Naldrett, A. J. Pt-190-Os-186 and Re-187-Os-187 systematics of the Sudbury Igneous Complex, Ontario. *Geochim. Cosmochim. Acta* **2002**, *66*, 273–290.
(48) Mathur, R.; Ruiz, J.; Tornos, F. Age and sources of the ore at Tharsis and Rio Tinto, Iberian Pyrite Belt, from Re-Os isotopes. *Miner. Deposita.* **1999**, *34*, 790–793.
(49) Rauch, S.; Hemond, H. F.; Peucker-Ehrenbrink, B. Recent changes in platinum group element concentrations and osmium isotopic composition in sediments from an urban lake. *Environ. Sci. Technol.* **2004**, *38*, 396–402.

ES901887F